Emission spectrum of a harmonically trapped two-level atom

Hong Guo[1,2,3,*] and Li-yan Zhao[1,†]
[1]*College of Physical Science and Technology, Huazhong Normal University, Wuhan 430079, China*
[2]*State Key Laboratory of Magnetic Resonance and Atomic and Molecular Physics, Wuhan Institute of Physics and Mathematics, Chinese Academy of Sciences, Wuhan 430071, China*
[3]*Center for Cold Atom Physics, Chinese Academy of Sciences, Wuhan 430071, China*
(Received 26 October 2005; published 26 May 2006)

We investigated theoretically the emission spectrum for a harmonically trapped two-level atom; our study is not limited in Lamb-Dicke approximation. We have shown that the effects of the atomic motion on the emission spectrum are dependent on the initial state of the system, the Lamb-Dicke parameter η, and the detuning parameter.

DOI: 10.1103/PhysRevA.73.053822 PACS number(s): 42.50.Dv, 32.80.Pj

I. INTRODUCTION

Much attention has been paid to spectra in the last decades; the wide investigation of the emission spectra [1–5] has revealed many nonclassical effects in the physical process of atom-radiation field interaction, including the successfully observed vacuum Rabi splitting [6]. It has been shown [7] that the emission spectrum of a stationary two-level atom interacting with one mode field is sensitive to the relative phase between the atomic dipole and the cavity field, for a certain choice of the relative phase, the spectrum can be an asymmetric two-peaked structure; the quantum state of radiation field for such a system can be recovered from the resonance fluorescence spectrum in some appropriate conditions [8].

Nevertheless, the atomic motion is unavoidable, and it could affect the atom-field interaction. The effects have been illustrated by many facts, such as spontaneous emission spectrum from an atom interacting with a standing-wave cavity mode [9], resonance fluorescence from a trapped atom [10], the dynamics of a trapped atom [11], etc. Compared with the stationary two-level atom, the atomic motion alters the decoherence and relaxation rates especially under the condition of certain atomic mass and resonant frequency [12]. With the rapid development of the atomic or ionic trapping technique, the system which consists of the atomic ions that are confined in electromagnetic traps and manipulated with laser beams is one of the most promising candidates for quantum information processing [13]. The nonclassical states of the trapped particle, such as the Fock state, squeezed state, coherent state, and the so-called Schrodinger-cat state, have been accomplished in experiments [14–16]. It is also possible to generate dark SU(2) coherent states of the center-of-mass (c.m.) motion of the trapped ion [17] and an entanglement state of two trapped ions [18]. The signal-to-noise ratio in spectroscopy of atoms can be enhanced using entanglement in the trapped particles [19].

However, most of the schemes are based on the Lamb-Dicke (LD) regime, which requires that the atom's motional excursion be much smaller than the laser wavelength, i.e., $\eta \ll 1$. In fact, the LD limit is not rigorously satisfied and the atomic oscillating motion is not limited to the LD limit. Indeed, it could be helpful to reduce the noise in the trap and improve the cooling rate [20] to use the laser-atom interaction outside the LD limit. The preparation of some pure state of the c.m. motion of a trapped atom (ion) is possible theoretically and experimentally [21,22] outside the LD limit. It has been shown [23] that the quantum motion of the trapped atom significantly influences the quantum fluctuations and the squeezing of fluorescence light field for atomic localization conditions far from the LD limit.

Recently, we investigated the effects of the atomic c.m. motion on the emission spectrum of a two-level harmonically oscillating atom driven by a resonant standing-wave field with a LD parameter nearly in LD approximation [24]. In this work, we will further study the emission spectrum of a harmonically trapped two-level atom driven by a running-wave field without a LD approximation. When the atom-field coupling constant λ, the interaction time T and the atomic decay rate γ satisfy the following inequalities [8]

$$\lambda \gg \frac{1}{T} \gg \gamma, \tag{1}$$

the spontaneous process can be negligible. In this case, the photon emitted by the atom into the cavity mode is likely to be repeatedly absorbed and re-emitted. The effect of recoil on the atom due to absorbing and emitting photons is nearly counteractive in a running-wave field [25], so we can neglect the effect of the recoil on average.

The present paper is organized as follows. In Sec. II, we derive the effective Hamiltonian of the system under consideration and present the atomic emission spectrum. In Sec. III, we discuss the emission spectrum in different initial states of the system. In Sec. IV, our results are presented.

II. THE MODEL

We consider a two-level atom undergoing a one-dimensional harmonic vibrational motion in the x direction and driven by a running wave inside an ideal cavity, in the rotating-wave approximation, the Hamiltonian for the system is (we use $\hbar = 1$)

*Electronic address: guohong@phy.ccnu.edu.cn
†Electronic address: eternalzly@etang.com

$$\hat{H}_0 = \omega_c \hat{b}^\dagger \hat{b} + \nu \hat{a}^\dagger \hat{a} + \omega_a \frac{\hat{\sigma}_z}{2}, \tag{2}$$

$$\hat{H}_I = \lambda \hat{\sigma}_+ \hat{b} e^{ik_c \hat{x}} + \text{H.c.} \tag{3}$$

Here, $\hat{H}_0$ is the free Hamiltonian of the atom and the radiation field, and $\hat{H}_I$ describes the interaction, $\hat{b}^\dagger$ and $\hat{b}$ are the creation and annihilation operators for the radiation field, $\hat{a}^\dagger$ and $\hat{a}$ are the creation and annihilation operators of the atomic vibrational quanta with frequency ν, $\hat{\sigma}_+$ ($\hat{\sigma}_-$) is the raising (lowering) operator of the atomic internal state, $\hat{\sigma}_z$ is the usual Pauli matrix, ω_c and ω_a are the field frequency and the atomic transition frequency, respectively, $k_c = \omega_c / c$, λ is the atom-field coupling constant. The operator $\hat{x}$ describes the position of the center-of-mass motion, which can be given as $\hat{x} = \sqrt{\hbar / 2\mu\nu}(\hat{a}^\dagger + \hat{a})$, μ is the atomic mass. When the field is resonant with the jth red sideband (blue sideband), $\omega_c = \omega_a - j\nu$ ($\omega_c = \omega_a + j\nu$), in the interaction picture, we disregard the rapidly oscillating terms and the interaction Hamiltonian becomes

$$\hat{H}_I = \hat{\sigma}_+ \hat{b} \hat{G}^j \hat{a}^j + \text{H.c.} \quad [\hat{H}_I = \hat{\sigma}_+ \hat{b} (\hat{a}^\dagger)^j \hat{G}^j + \text{H.c.}] \tag{4}$$

with

$$\hat{G}^j = \lambda e^{-\eta^2/2} \sum_{l=0}^{\hat{M}} \frac{(i\eta)^{(2l+j)} \hat{M}!}{(j+l)!\, l!\, (\hat{M}-l)!}. \tag{5}$$

Here, $\hat{M} = \hat{a}^\dagger \hat{a}$ is the occupation number of the atomic oscillating motion, η is the Lamb-Dicke parameter, $\eta = k_c \sqrt{\hbar / 2\mu\nu}$.

If the half-band-width of the spectrometer Γ is much larger than the atomic decay rate γ, the time-dependent physical spectrum $S(\omega)$ of the radiation field emitted by a harmonically trapped two-level atom inside an ideal cavity can be expressed as [26]

$$S(\omega) = 2\Gamma \int_0^T dt_1 \int_0^T dt_2 e^{-(\Gamma - i\omega)(T - t_1) - (\Gamma + i\omega)(T - t_2)} \times \langle \psi(0) | \hat{\sigma}_+(t_1) \hat{\sigma}_-(t_2) | \psi(0) \rangle, \tag{6}$$

where $|\psi(0)\rangle$ is the initial state of the atom-field system, $|\psi(0)\rangle = |\psi_a\rangle \otimes |\psi_a'\rangle \otimes |\psi_f\rangle$, $|\psi_a\rangle$ is the atomic internal state, $|\psi_a'\rangle$ and $|\psi_f\rangle$ are the initial states of atomic c.m. motion and the radiation field, respectively.

III. THE ATOMIC EMISSION SPECTRUM

We now assume that the atomic internal state $|\psi_a\rangle$ is initially in coherent superposition of the excited state $|e\rangle$ and the ground state $|g\rangle$, i.e., $|\psi_a\rangle = \cos\theta/2 |g\rangle + \sin\theta/2 e^{i\Phi} |e\rangle$ ($0 \leqslant \theta \leqslant \pi, -\pi < \Phi \leqslant \pi$), the field and the c.m. motion are both in the coherent superposition state of the number states, $|\psi_f\rangle = \Sigma_n^\infty F_n |n\rangle$, $|\psi_a'\rangle = \Sigma_m^\infty D_m |m\rangle$, the initial state of the system is given by the expression

$$|\psi(0)\rangle = \sum_{n,m=0}^{\infty} D_m F_n \left(\cos\frac{\theta}{2} |n,g,m\rangle + \sin\frac{\theta}{2} e^{i\Phi} |n,e,m\rangle \right). \tag{7}$$

When we tune the laser to the jth red sideband, i.e., $\omega_c = \omega_a - j\nu$ ($j = 0,1,2,3\ldots$), the emission spectrum $S(\omega)$ of a harmonically trapped two-level atom is given by the expression

$$\begin{aligned} S(\omega) = \frac{\Gamma}{4} \sum_{n=0,m=j}^{\infty} \Bigg[\Bigg| & \left(i^j F_{n+1} D_{m+j} \cos\frac{\theta}{2} + F_n D_m \sin\frac{\theta}{2} e^{i\Phi} \right) \\ & \times \Omega(-\beta_{n,m}^j, \beta_{n-1,m-j}^j) \\ & + \left(-i^j F_{n+1} D_{m+j} \cos\frac{\theta}{2} + F_n D_m \sin\frac{\theta}{2} e^{i\Phi} \right) \\ & \times \Omega(\beta_{n,m}^j, \beta_{n-1,m-j}^j) \Bigg|^2 + (-\beta_{n-1,m-j}^j \to \beta_{n-1,m-j}^j) \Bigg] \\ & + \frac{\Gamma}{2} \sum_{m=0}^{j-1} \sum_{n=0}^{\infty} \Bigg| \left(i^j F_{n+1} D_{m+j} \cos\frac{\theta}{2} + F_n D_m \sin\frac{\theta}{2} e^{i\Phi} \right) \\ & \times \Omega(-\beta_{n,m}^j, 0) + \Bigg(-i^j F_{n+1} D_{m+j} \cos\frac{\theta}{2} \\ & + F_n D_m \sin\frac{\theta}{2} e^{i\Phi} \Bigg) \Omega(\beta_{n,m}^j, 0) \Bigg|^2, \end{aligned} \tag{8}$$

where $(-\beta_{n-1,m-j}^j \to \beta_{n-1,m-j}^j)$ is denoted as substituting $\beta_{n-1,m-j}^j$ for $-\beta_{n-1,m-j}^j$, and

$$\Omega(x,y) = \frac{\exp[i(\omega - \omega_a + x + y)T] - \exp(-\Gamma T)}{\Gamma + i(\omega - \omega_a + x + y)}, \tag{9}$$

$$\beta_{n,m}^j = |g_m^j| \sqrt{\frac{(n+1)(m+j)!}{m!}}, \tag{10}$$

$$g_m^j = \lambda e^{-\eta^2/2} \sum_{l=0}^{m} \frac{(i\eta)^{2l+j} m!}{(j+l)!\, l!\, (m-l)!}. \tag{11}$$

If we tune the laser to the jth blue sideband, then

$$\begin{aligned} S(\omega) = \frac{\Gamma}{4} \sum_{n=0,m=j}^{\infty} \Bigg[\Bigg| & \left(i^j F_{n+1} D_{m-j} \cos\frac{\theta}{2} + F_n D_m \sin\frac{\theta}{2} e^{i\Phi} \right) \\ & \times \Omega(-\beta_{n,m-j}^j, \beta_{n-1,m}^j) \\ & + \left(-i^j F_{n+1} D_{m-j} \cos\frac{\theta}{2} + F_n D_m \sin\frac{\theta}{2} e^{i\Phi} \right) \\ & \times \Omega(\beta_{n,m-j}^j, \beta_{n-1,m}^j) \Bigg|^2 + (-\beta_{n-1,m}^j \to \beta_{n-1,m}^j) \Bigg] \\ & + \Gamma \sum_{m=0}^{j-1} \sum_{n=0}^{\infty} \left| F_n D_m \sin\frac{\theta}{2} \right|^2 \\ & \times (|\Omega(-\beta_{n-1,m}^j, 0)|^2 + |\Omega(\beta_{n-1,m}^j, 0)|^2). \end{aligned} \tag{12}$$

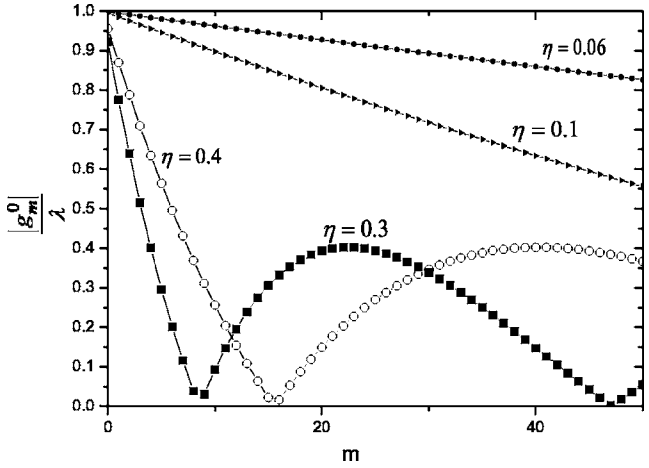

FIG. 1. The effective coupling constant $|g_m^0|$ is shown as a function of the atomic c.m. motional occupation number m, when $j=0$.

When $j=0$, i.e., $\omega_c=\omega_a$, the emission spectrum is still sensitive to the relative phase between the atomic dipole and the field, regardless of the initial state of the atomic motion; however, in the case of $j\neq 0$, the atomic spectrum would lose phase sensitivity provided that the atomic motion in Fock state or mixed state, furthermore the atomic spectrum is related with not only the relative phase between the atomic dipole and the field but also the phase of the atomic c.m. motion, supposing the atomic c.m. motion is in coherent state, as shown in Fig. 12(2).

A. The radiation field in Fock state

For simplicity, we discuss the emission spectrum for $j=0$ and $j=1$, i.e., the driving field is resonant with the atom and with the first red (blue) sideband, respectively. We consider that the atom is initially in an excited state, when the atomic c.m. motion and the field are both in Fock states, for $j=0$, the atomic emission spectrum has a four-peak structure, the four peaks are located at

$$\omega_a \pm |g_m^0|(\sqrt{n+1}-\sqrt{n}), \quad \omega_a \pm |g_m^0|(\sqrt{n+1}+\sqrt{n}). \quad (13)$$

As shown in Fig. 1, when the atomic c.m. occupation number $m=0$, the effective coupling constant $|g_0^0|$ is $\lambda e^{-\eta^2/2}$, it is beyond the LD limit that the vacuum fluctuation of the quantized atomic motion is not negligible. Moreover, $|g_m^0|$ displays the nonperiodic "oscillation" with increasing m, the average period of oscillation decreases along with the increase of a LD parameter, and the maximum of $|g_m^0|$ is smaller than the atom-field coupling constant λ; for appropriate occupation number, $|g_m^0| \ll \lambda$. Consequently, as shown in Fig. 2, compared with the stationary atomic spectra, a nearness of the two sidebands can be seen even when the c.m. motion is in a vacuum state. The atomic emission spectrum is sensitive to the occupation number of the atomic motion. When the occupation number m is increased, first, the two sidebands move toward each other and even overlap

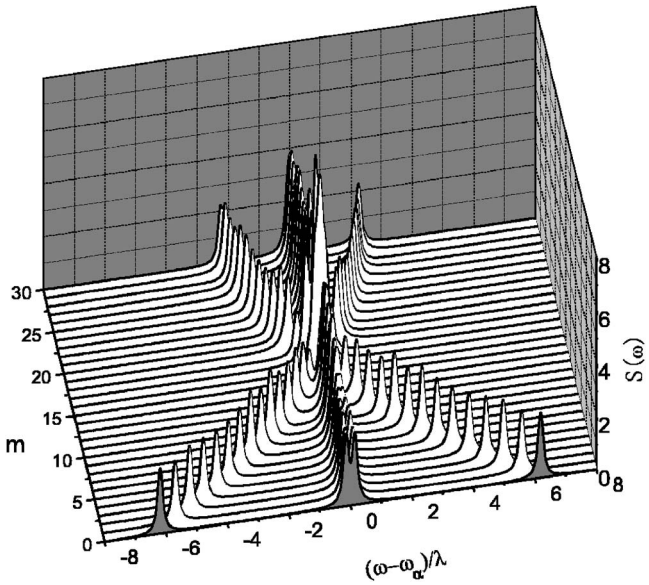

FIG. 2. The emission spectrum, the field is in photon number state, the atomic c.m. motion is in Fock state, $j=0$, $\theta=\pi$, $\eta=0.3$, $n=10$, $T=40/\lambda$, $\Gamma=0.1\lambda$.

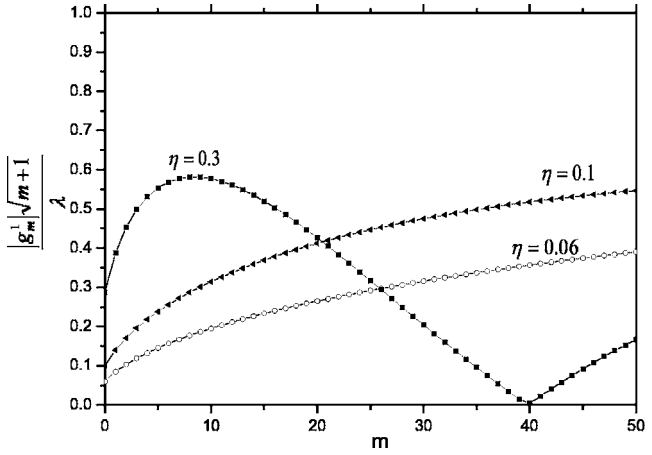

FIG. 3. Same as Fig. 1, but $j=1$ (red sideband or blue sideband).

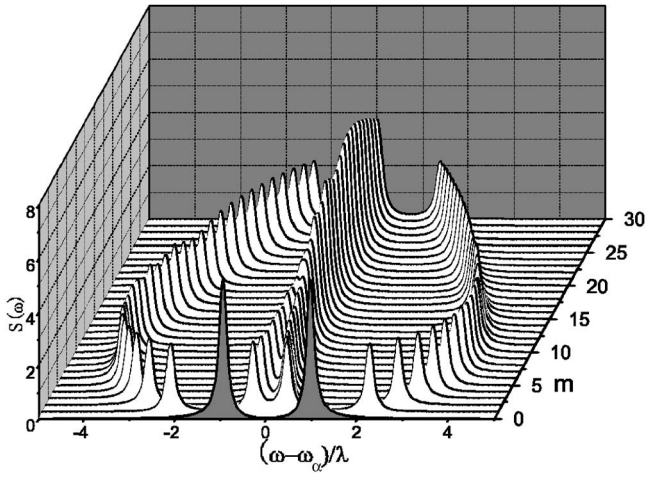

FIG. 4. Same as Fig. 2, but $j=1$ (red sideband).

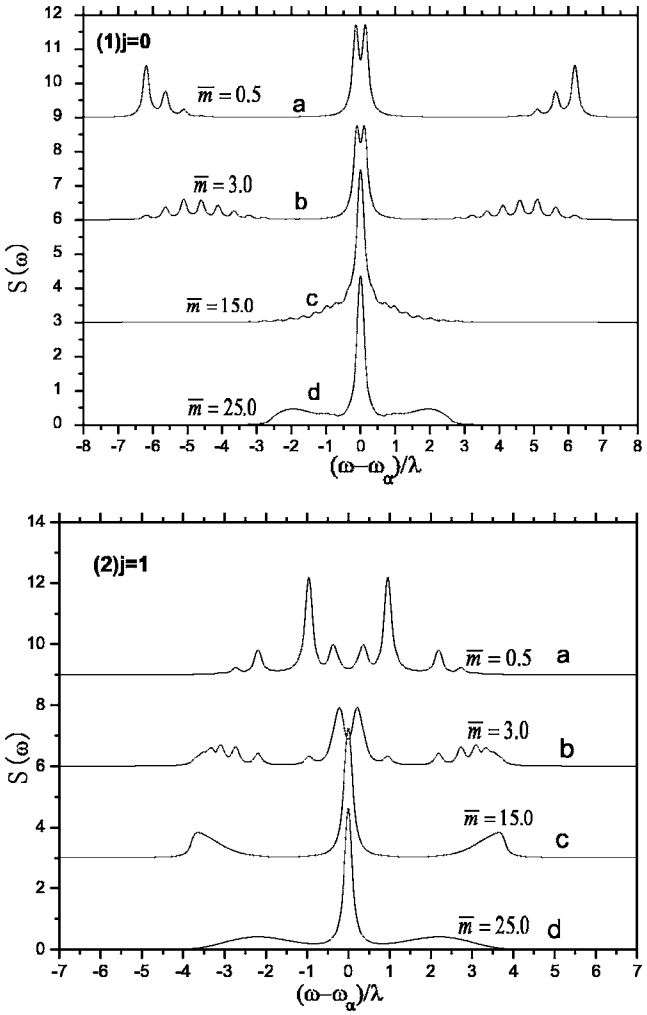

FIG. 5. Figure 1 is same as Fig. 2, but the atomic c.m. motion is in coherent state, Fig. 2 is the same as Fig. 1, but $j=1$, a $S(\omega)+9.0$; b $S(\omega)+6.0$; c $S(\omega)+3.0$; d $S(\omega)$.

around ω_a; that is, the spectra could appear approximately at one peak, then they recede from each other. However, in the LD limit (or nearly in the LD limit), $|g_m^0| \approx \lambda[1-\eta^2/2(1+2m)]$, hence the two sidebands move toward each other with increasing m, which conforms to [25], since the effective Hamiltonian of the system in this case is almost same as the Hamiltonian in [25].

When the driving field is tuned to the first red sideband, the peaks are located at

$$\omega_a \pm (|g_m^1|\sqrt{(n+1)(m+1)} - |g_{m-1}^1|\sqrt{nm});$$

$$\omega_a \pm (|g_m^1|\sqrt{(n+1)(m+1)} + |g_{m-1}^1|\sqrt{nm}). \quad (14)$$

When the atomic c.m. motion is in the vacuum state, the emission spectrum is two-peak structure instead of four visible peaks, even when the field is not in a vacuum state. As shown in Fig. 3, for $m=0$, the effective coupling constant $|g_0^1| = \lambda e^{-\eta^2/2}\eta$ is much smaller than the atom-field coupling constant λ. As shown in Fig. 4, outside the LD limit, with the increase of the occupation number m, the two sidebands first recede from each other, then they move close together, since the effective coupling constant $|g_m^1|\sqrt{m+1}$ exhibits a nonperiodic oscillation which is very different from the situation for $j=0$. In the LD limit, with increasing m the two sidebands of the atomic spectra always move away each other, because the effective coupling constant $|g_m^1|\sqrt{m+1}$ grows slowly with the occupation number m.

If the driving field is tuned to the first blue sideband, the locations of the peaks are

$$\omega_a \pm [|g_{m-1}^1|\sqrt{(n+1)m} - |g_m^1|\sqrt{n(m+1)}],$$

$$\omega_a \pm [|g_{m-1}^1|\sqrt{(n+1)m} + |g_m^1|\sqrt{n(m+1)}]. \quad (15)$$

Generally, the atomic spectra are very similar to the case of the first red sideband. However, when the field and the atomic motion are both in a vacuum state, only one peak located at ω_a appears in the atomic spectra, i.e., vacuum "Rabi splitting" could not be observed due to the atomic c.m motion under this condition.

When the atomic c.m. motion is in a coherent state, the atomic spectra depend on both the effective coupling constant and the occupation number distribution. Outside the LD limit, as seen in Fig. 5, for $j=0$, when the mean occupation number is small, the two sidebands of the emission spectra

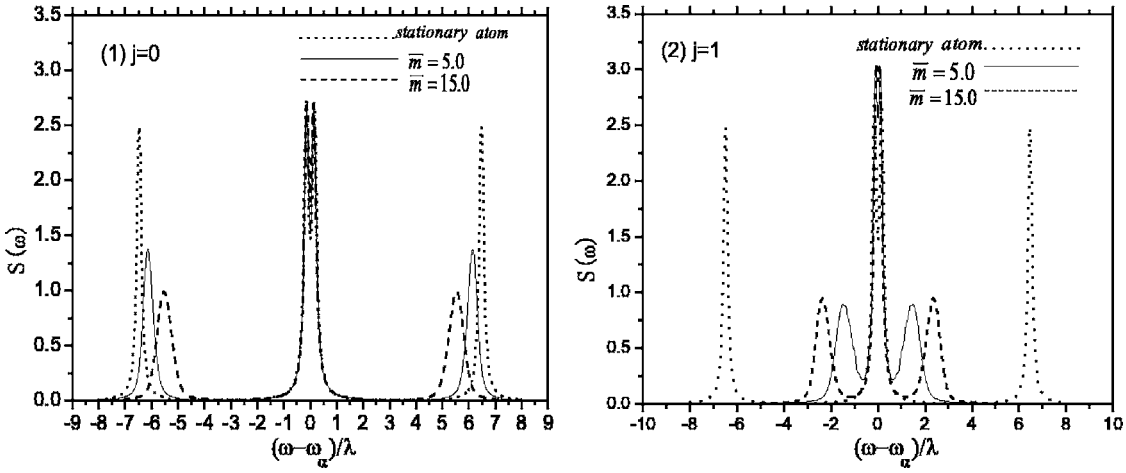

FIG. 6. Same as Fig. 5, but $\eta=0.1$.

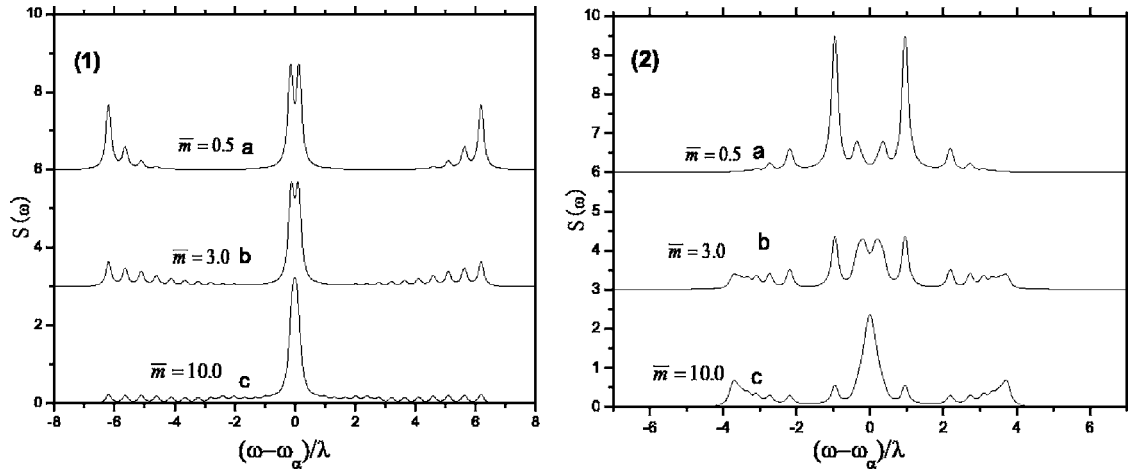

FIG. 7. Figure 1 is the same as Fig. 2, but the atomic c.m. motion is in thermal state, Fig. 2 is the same as Fig. 1, but $j=1$, a $S(\omega)+6.0$; b $S(\omega)+3.0$; c $S(\omega)$.

evolve into a complicated multipeak structure because of the rapid decreasing of $|g_m^0|$ with the increasing occupation number m, and every small peak's height is proportional to $|D_m|^2$. For sufficiently large $\bar{m}$, the small peaks coalesce, the two sidebands appear again; for $j=1$, the multipeak structure instead of a four-peak emerges due to rapid increasing of $|g_m^1|\sqrt{m+1}$ with increasing small m. When $\bar{m}$ is increased further, the two sidebands are formed and the atomic spectrum is sensitive to the mean occupation number. In the LD limit, for $j=1$, when $\bar{m}$ is sufficiently large with increasing $\bar{m}$, the two sidebands recede from each other, heighten, and narrow. However, compared with the stationary resonant spectra, the two sidebands broaden and move together. Yet, for $j=0$, it is quite different, with increasing $\bar{m}$, the two sidebands move toward each other and broaden, as shown in Fig. 6.

When the atomic c.m. motion is in thermal state, the main contribution to the emission spectra is the small occupation number states due to the broad thermal distribution with maximum at $m=0$ and dominant weights at small occupation number states. Consequently, outside the LD limit, as shown in Fig. 7, the emission spectrum is always multipeak due to the atomic motion except $\bar{m}=0$. In the LD limit, as shown in Fig. 8, when $j=0$, compared with the atomic c.m. motion in coherent state, for the same $\bar{m}$, the sidebands are broader, since the fluctuation of thermal state increases more quickly than coherent state with increasing $\bar{m}$, but for $j=1$, the atomic spectrum is quite different.

B. The field in coherent state

We consider the radiation field is in coherent state, outside the LD limit, when the atomic c.m. motion is in Fock state, for $j=0$, as shown in Fig. 9, when the atomic c.m. motion is in a vacuum state, the emission spectrum is very similar to that of stationary atom. With increasing m, the small peaks coalesce to two sidebands, when m is further increased, the two sidebands first narrow and move toward each other, then broaden, and recede from each other. Compared with Fig. 2, for the same occupation number, the two sidebands are broadened. For $j=1$, as shown in Fig. 10, with increasing m, the two sidebands first broaden and move away from each

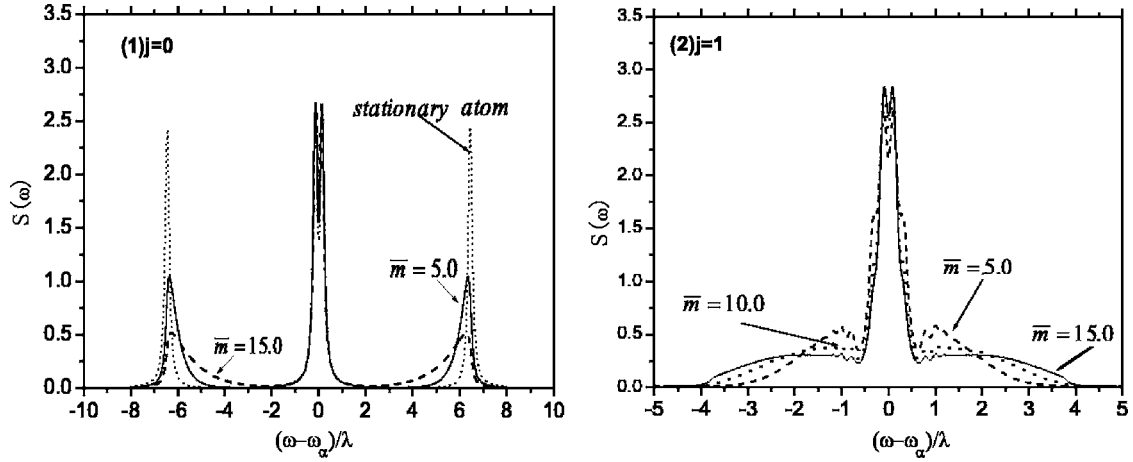

FIG. 8. Same as Fig. 7, but $\eta=0.1$.

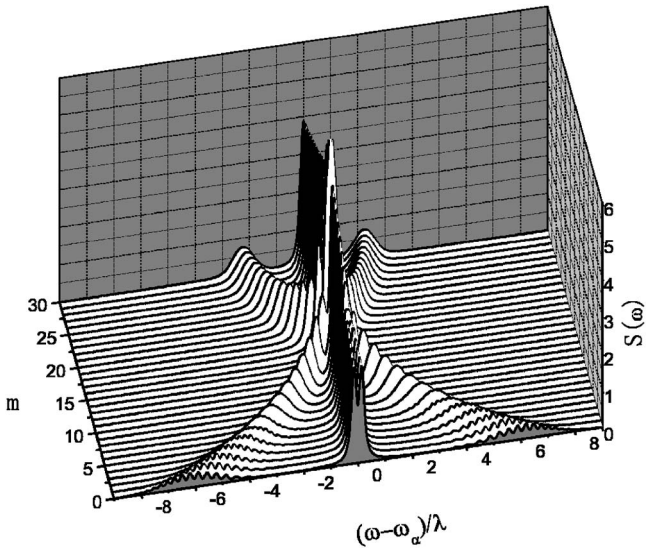

FIG. 9. Same as Fig. 2, but the radiation field is coherent state, $\bar{n}=10.0$.

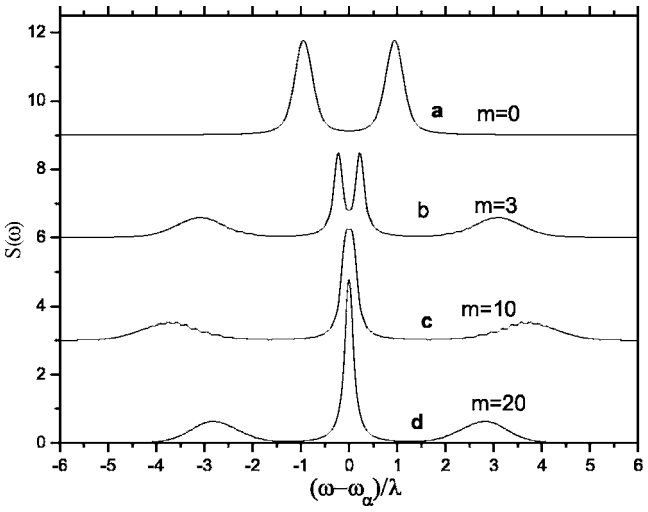

FIG. 10. Same as Fig. 4, but the radiation field is coherent state $\bar{n}=10.0$, a $S(\omega)+9.0$; b $S(\omega)+6.0$; c $S(\omega)+3.0$; d $S(\omega)$.

other, then narrow and move toward each other. Compared with Fig. 4, the sidebands are also broadened for the same occupation number m.

When the cavity field is initially in coherent state, the emission spectrum for the atomic c.m. motion in coherent state is similar to that of the atomic c.m. motion in Fock state except for the widened sidebands.

When the atomic motion is thermal state, as shown in Fig. 11, if the field is resonant with the atom, the location of the two sidebands is not as sensitive to the intensity of the atomic motion, but the sidebands become wider and lower with the increasing mean occupation number $\bar{m}$. If the field is tuned to the first red sideband, at first the atomic emission spectrum exhibits six peaks, with increasing $\bar{m}$, the outermost peaks move away and broaden, the peaks located at $\omega_a \pm |g_0^1| \sqrt{\bar{n}+1}$ decrease due to the decreasing weight of vacuum state, the central two peaks move together and then overlap.

In the LD limit, if the atomic motion is in Fock state or coherent state, with increasing $\bar{m}$, when the driving field is resonant with the first red (blue) sideband, the two sidebands recede from each other, the peak-height of the sideband decreases. When the field is resonant with the atom, the sidebands move together and heighten, as shown in Fig. 12.

IV. CONCLUSION

The effective Hamiltonian of the system is different for different detuning parameters. Hence, the emission spectrum of a harmonically trapped two-level atom depends on not only the initial state of the system and the LD parameter η, but also the detuning parameter. When $j=0$, the atomic c.m. motion merely affects the coupling strength between the atom and the driving field. Consequently, the phase sensitivity of the two-level atomic emission spectrum is not affected by the atomic c.m. motion. When $j=1$, the change of the atomic internal state brings the changes of the field and the atomic c.m. motion, thereby, the phase sensitivity of the emission spectrum depends on the atomic c.m. motion. In

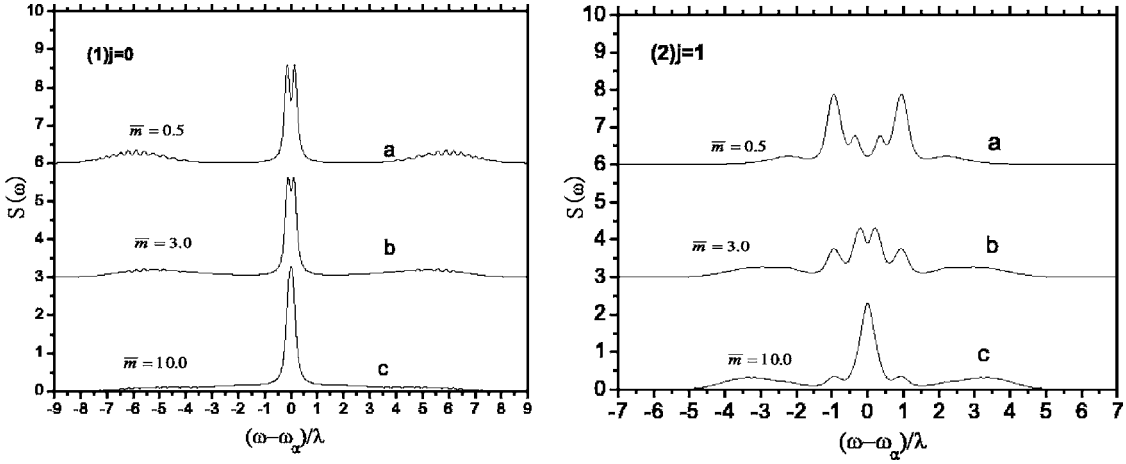

FIG. 11. Same as Fig. 7, but the field is in coherent state $\bar{n}=10.0$.

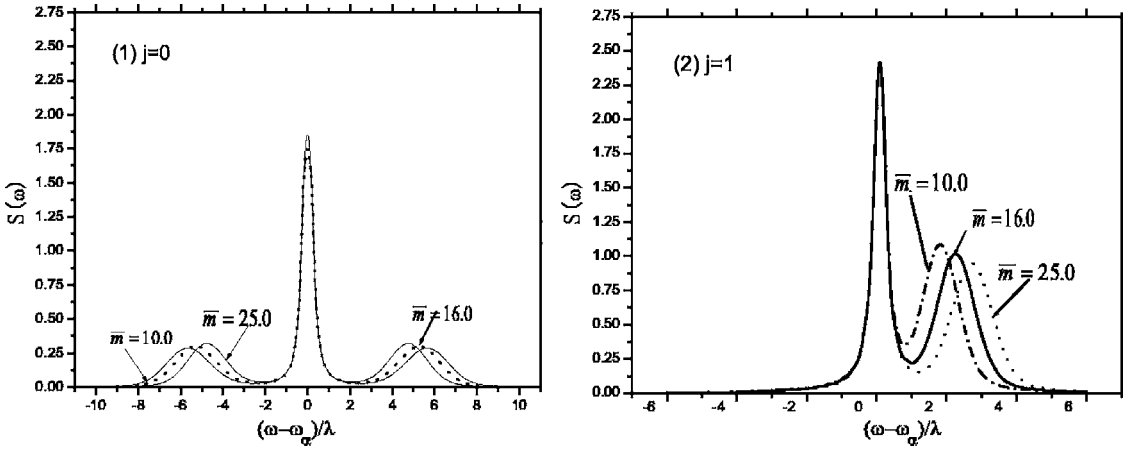

FIG. 12. The atomic c.m. motion and the radiation field are in coherent state $\bar{n}=10.0$, $\theta=\pi/2$, the relative phase of the atomic c.m. motion, the radiation field and the atomic dipole is $\pi/2$; $\eta=0.1$, $\Gamma=0.2\lambda$, $T=20/\lambda$.

summary, the shape of the emission spectrum for a harmonically trapped two-level atom may be controlled via the LD parameter η, the detuning parameter, and the atomic c.m. motion. There may be potential applications in the precision measurement.

ACKNOWLEDGMENTS

The author acknowledge Professor G. X. Li for helpful discussions and financial support from the Natural Science Foundation of China (Grant No. 60478049), the Key Research Project of the National Ministry of Education.

[1] T. Nasreen and M. S. K. Razmi, J. Opt. Soc. Am. B **10**, 1292 (1993).
[2] M. M. Ashraf, Phys. Rev. A **50**, 741 (1994).
[3] N. B. Narozhny, J. J. Sanchez-Mondragon, and J. H. Eberly, Phys. Rev. A **23**, 236 (1981).
[4] J. J. Sanchez-Mondragon, N. B. Narozhny, and J. H. Eberly, Phys. Rev. Lett. **51**, 550 (1983).
[5] J. Gea-Banacloche, R. R. Schlicher, and M. S. Zubairy, Phys. Rev. A **38**, 3514 (1988); G. S. Agarwal, Phys. Rev. Lett. **67**, 980 (1991).
[6] R. J. Thompson, G. Rempe, and H. J. Kimble, Phys. Rev. Lett. **68**, 1132 (1992).
[7] K. Zaheer and M. S. Zubairy, Phys. Rev. A **39**, 2000 (1989).
[8] M. S. Zubairy, Phys. Rev. A **57**, 2066 (1998).
[9] W. Ren and H. J. Carmichael, Phys. Rev. A **51**, 752 (1995).
[10] J. I. Cirac, R. Blatt, A. S. Parkins, and P. Zoller, Phys. Rev. A **48**, 2169 (1993).
[11] F. L. Semiäo, A. Vidiella-Barranco, and J. A. Roversi, Phys. Rev. A **66**, 063403 (2002); A. Ray, Phys. Rev. A **69**, 033806 (2004); A. Joshi and M. Xiao, Opt. Commun. **232**, 273 (2003); H. Moya-Cessa, A. Vidiella-Barranco, J. A. Roversi, Dagoerto S. Freitas, and S. M. Dutra, Phys. Rev. A **59**, 2518 (1999).
[12] S. Shresta and B. L. Hu, Phys. Rev. A **68**, 012110 (2003).
[13] D. Leibfried, E. Knill, S. Seidelin, J. Britton, R. B. Blakestad, J. Chiaverini, D. B. Hume, W. M. Itano, J. D. Jost, C. Langer, R. Ozeri, R. Reichle, and D. J. Wineland, Nature (London) **438**, 639 (2005).
[14] D. Leibfried, D. M. Meekhof, B. E. King, C. Monroe, W. M. Itano, and D. J. Wineland, Phys. Rev. Lett. **77**, 4281 (1996).
[15] C. Monroe, D. M. Meekhof, and B. E. King, Science **272**, 1131 (1996).
[16] D. M. Meekhof, C. Monroe, B. E. King, W. M. Itano, and D. J. Wineland, Phys. Rev. Lett. **76**, 1796 (1996).
[17] Z. Kis, W. Vogel, L. Davidovich, and N. Zagury, Phys. Rev. A **63**, 053410 (2001).
[18] G. X. Li, S. P. Wu, and G. M. Huang, Phys. Rev. A **71**, 063817 (2005).
[19] D. Leibfried, M. D. Barrett, T. Schaetz, J. Britton, J. Chiaverini, W. M. Itano, J. D. Jost, C. Langer, and D. J. Wineland, Science **304**, 1476 (2004); P. O. Schmidt, T. Rosenband, C. Langer, W. M. Itano, J. C. Bergquist, and D. J. Wineland, *ibid.* **309**, 749 (2005).
[20] D. Stevens, J. Brochard, and A. M. Steane, Phys. Rev. A **58**, 2750 (1998); A. Steane, Appl. Phys. B: Lasers Opt. **64**, 623 (1997); D. F. V. James, *ibid.* **66**, 181 (1998); G. Morigi, J. I. Cirac, M. Lewenstein, and P. Zoller, Europhys. Lett. **39**, 13 (1997).
[21] P. A. Barton, C. J. S. Donald, D. M. Lucas, D. A. Stevens, A. M. Steane, and D. N. Stacey, Phys. Rev. A **62**, 032503 (2000).
[22] L. F. Wei, Y. X. Liu, and F. Nori, Phys. Rev. A **70**, 063801 (2004).
[23] R. L. de Matos Filho and W. Vogel, Phys. Rev. A **49**, 2812 (1994).
[24] H. Guo and L. Y. Zhao, Acta Phys. Sin. **54**, 4723 (2005).
[25] J. S. Peng and G. X. Li, *Introduction to Modern Quantum Optics* (World Scientific Press, Singapore, 1998), Chap. 17.
[26] J. H. Eberly and K. Wodkiewicz, J. Opt. Soc. Am. **67**, 1252 (1977).